ELECTRON CLOUD AND HEAT LOADS IN RUN 2

G. Iadarola*, B. Bradu, P. Dijkstall, L. Mether, G. Rumolo, A. Romano, G. Skripka, L. Tavian
CERN, Geneva, Switzerland

Abstract

During Run 2, the 25 ns bunch spacing was routinely used for proton physics operation at the LHC. With this bunch spacing, electron cloud effects are significantly more severe than with the 50 ns spacing, which had been used for luminosity production in Run 1. Beam-induced scrubbing allowed to mitigate the electron cloud formation enough to allow an effective exploitation of 25 ns beams for physics operation. Nevertheless, even after years of conditioning of the beam chambers, e-cloud effects remain very visible, affecting beam stability and beam quality preservation, and generating a significant heat load on the beam screens of the superconducting magnets. Surprisingly, the eight LHC arcs show very different behaviors, with the heat load being much higher for some of them (S12, S23, S78 and S81) compared to the others. In these sectors, the heat loads are very close to the nominal cooling capacity delivered by the corresponding cryoplant, which is a concern in view of the planned upgrade program. A dedicated interdepartmental Task Force has been formed to investigate this issue. This contribution summarizes the relevant observations and studies conducted during Run 2, the interventions planned for LS2 and briefly discusses prospects for Run 3.

INTRODUCTION

Electron cloud effects were identified among the main performance limitations for the Large Hadron Collider (LHC) already at the time of its design and construction [1].

Run 2 (2015-2018) marked an important milestone with respect to e-cloud effects in the LHC, since it was only in Run 2 that the nominal bunch spacing of 25 ns was used routinely for p-p physics operation. In Run 1 (2010-2013), the 50 ns bunch spacing had been used for most of the luminosity production fills [2–4]. With 50 ns bunch spacing, e-cloud effects are much less severe than with 25 ns [5].

The experience accumulated in Run 2 showed that beam-induced conditioning of the beam-chamber surfaces, often called "scrubbing", can significantly mitigate the e-cloud formation, to an extent that allows a satisfactory exploitation of 25 ns beams in physics operation. It was also observed that the conditioning is mostly preserved over long stops, in the regions where the beam vacuum is preserved. In particular, after Year-End Technical Stops (YETS), only about one day of reconditioning is necessary [6, 7].

Nevertheless, the conditioning accumulated over the entire Run 2 was not sufficient to effectively suppress the e-cloud formation. The impact of the e-cloud on the beams remained visible and large heat loads on the beam screens were measured especially in some sectors, as will be discussed in the following sections.

* Giovanni.Iadarola@cern.ch

EFFECTS ON THE BEAM

During the Long Shutdown 1 (LS1) the surfaces of most of the LHC beam chambers were exposed to air, including in particular all the beam screens in the arcs. Due to this, at the very beginning of Run 2, strong e-clouds were developing when injecting 25 ns beams, triggering violent transverse instabilities [6].

A long scrubbing period was required in order to recover an acceptable beam quality. The evolution of the beam quality during the scrubbing run is illustrated in Fig. 1. At the beginning only short bunch-trains could be circulated due to violent losses on the trailing bunches of the trains, caused by transverse instabilities. Over the scrubbing run, thanks to the conditioning effect of electrons bombarding the surfaces exposed to the beam, it was gradually possible to inject longer trains, still with visible beam losses. It was only after 12 days dedicated to scrubbing that the accumulated conditioning allowed achieving beam stability and therefore mitigating the losses.

Still, after the scrubbing run and during the entire Run 2, in order to keep the beams stable at 450 GeV it was necessary to use high chromaticity ($Q'_{x,y} \geq 15$) and high octupole settings ($I_{\mathrm{oct}} > 40$ A), together with the full performance of the LHC transverse feedback (high gain, large bandwidth settings). Even in this configuration weak instabilities still occasionally occured, causing no losses and a modest but detectable emittance blow-up on some of the bunches [8].

In order to preserve the beam lifetime at 450 GeV, the transverse tune settings needed to be optimized in order to better accommodate the large tune footprint generated by the e-cloud, the chromaticity and the octupoles as shown in Fig. 2 [9]. Even when the beam is kept stable the e-cloud causes a slow beam degradation, with observable losses and emittance blow-up. This is particularly visible when the beams are stored at 450 GeV for longer than usual (see Fig. 3).

Thanks to the increased beam rigidity, at 6.5 TeV the effects of the e-cloud on the beams are much weaker but still clearly visible. In particular the typical "e-cloud signature" is clearly visible on the bunch-by-bunch losses when the beams are colliding [10].

A curious effect was observed at the beginning of the 2016 run, when the beams were becoming unstable in the vertical plane after a few hours in collisions. The cause of this instability was found to be the e-cloud in the dipole magnets, which becomes more dense at the beam location when the intensity decreases due to luminosity burn-off. These instabilities disappeared when the bunch-train length

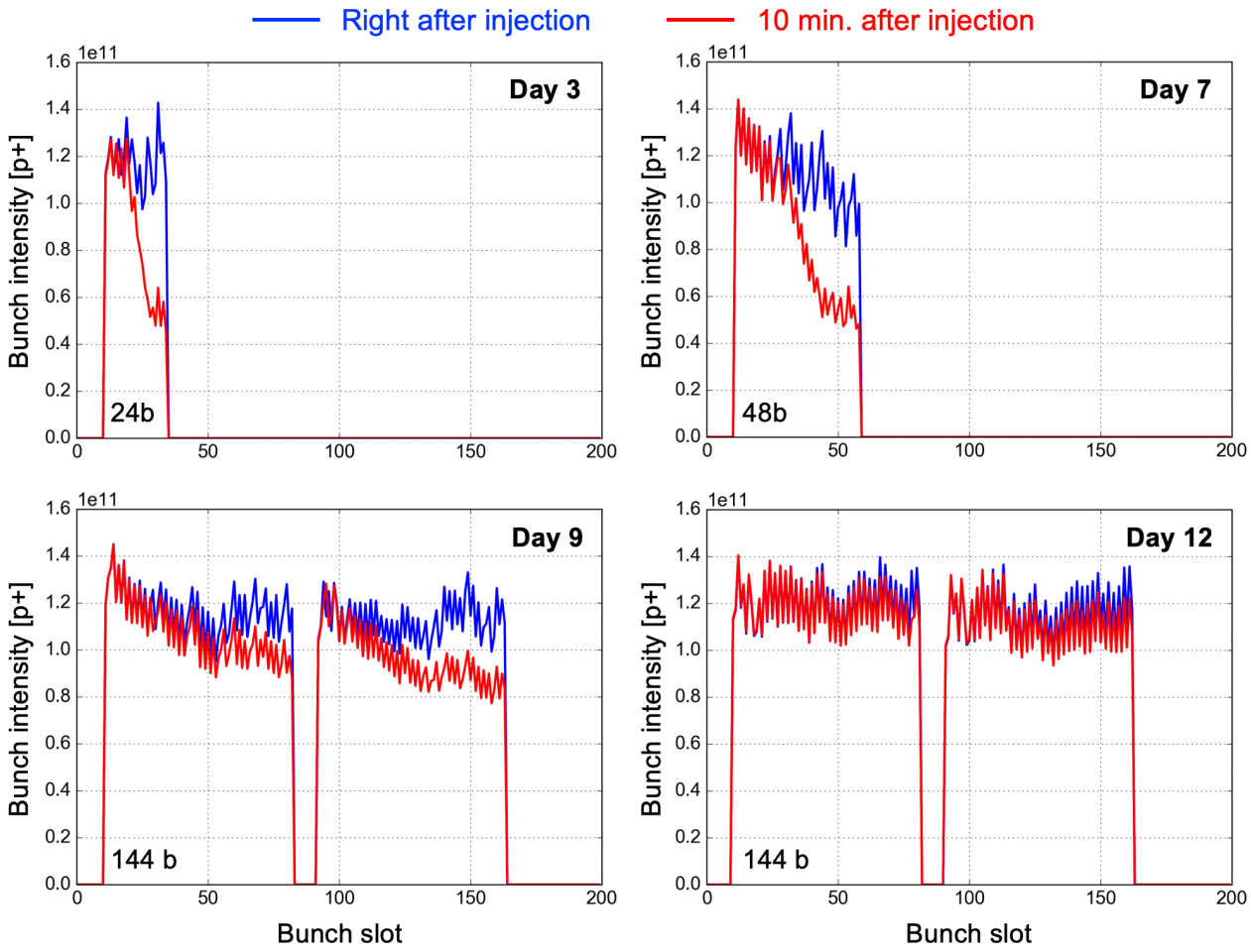

Figure 1: Intensity of bunches within an injected train measured right after the injection (in blue) and ten minutes after the injection (in red). The different subplots correspond to different moments during the 2015 scrubbing run with 25 ns beams. The day count excludes long stops due to faults, tests or other activities.

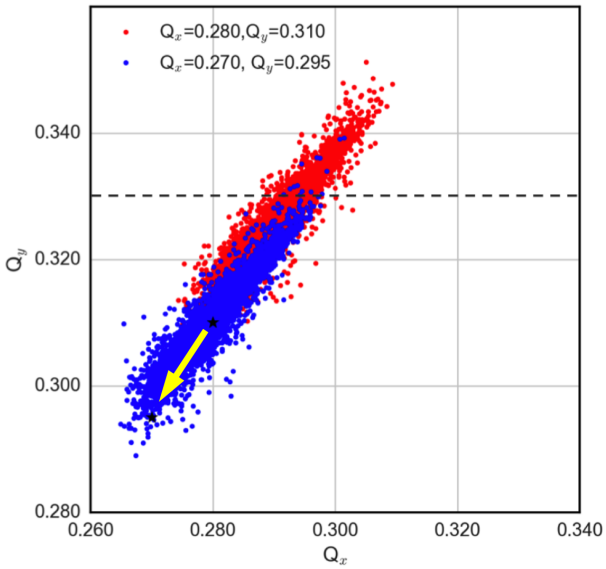

Figure 2: Tune footprints evaluated from PyECLOUD-PyHEADTAIL simulations for a LHC bunch at injection including the effect of octupoles powered at 26 A, chromaticity set at $Q'_{x,y} = 15$, and e-cloud in dipole and quadrupole magnets. The dashed line represents the third order resonance Qy =.33. Two tune settings are considered as indicated in the legend.

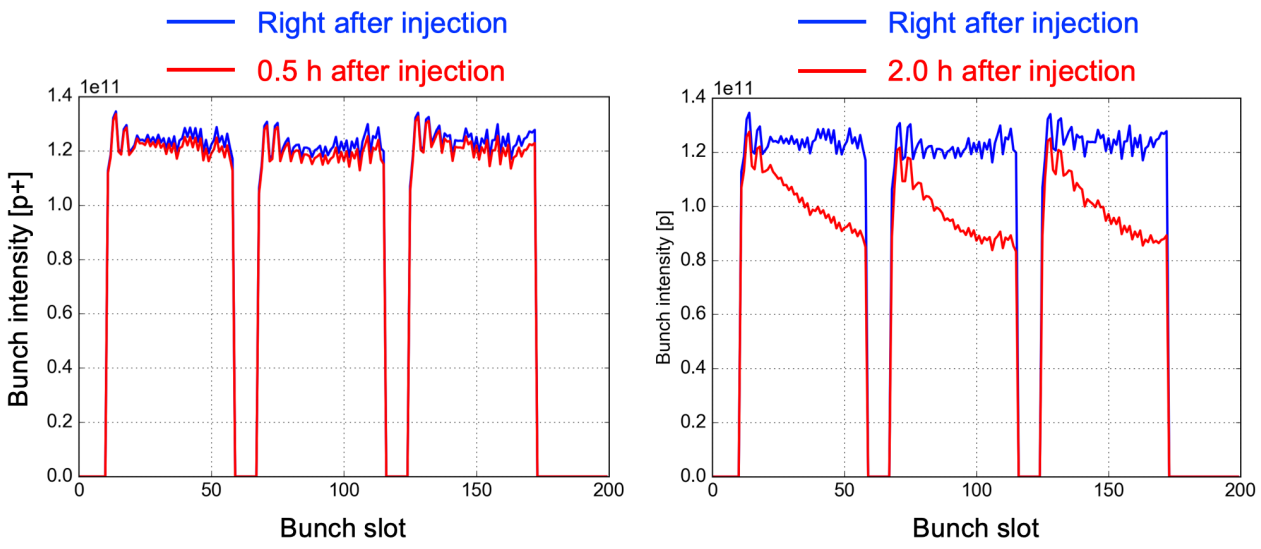

Figure 3: Intensity of bunches within an injected train for a fill in which the beam was kept at injection energy for a few hours (test performed during 2017 with optimized tune settings).

was reduced from 72 bunches to 48 bunches in order to profit from high-brightness beams (BCMS) available from the injectors [11]. More details on this effect can be found in [12].

HEAT LOADS ON THE ARC BEAM SCREENS

Issues, mitigation and evolution in Run 2

Electrons impacting on the beams screens of the arc superconducting magnets deposit a significant amount of energy. These heat loads need to be absorbed by the beam-screen cooling integrated in the LHC cryogenics system [1]. The largest heat loads were measured in 2015, when some of the arcs reached levels close to the design cooling capacity of 160 W/half-cell, as shown in Fig. 4. In particular it is possible to notice that in all sectors the heat loads were significantly larger than expected from impedance and synchrotron radiation.

Limitations due to the heat loads were encountered especially in 2015. At that time, transients in heat load occurring when the beams were injected, during the energy ramp and at the beam dump, were leading to large excursions on the temperature of the beam screens, reaching the "cryo-conditions" interlock levels (above which the beams are dumped and powering on the concerned superconducting circuit is removed) [13]. Two measures were deployed to address this problem:

1. After careful review the "Cryo-Maintain" interlock rules were modified to allow for larger transients. Originally the interlock triggered if the temperature of the helium in the beam screen circuit would exceed 30 K for 30 seconds. After the modification the interlock triggers only if the temperature exceeds 40 K for 30 minutes [14].

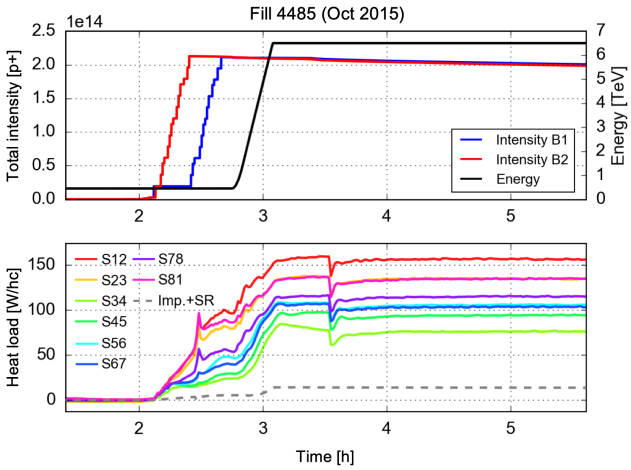

Figure 4: One of the physics fills during which the highest heat loads on the arc beam screens were observed. Top: intensity and energy of the circulating beams. Bottom: heat loads measured in the eight arcs (average per half-cell). The expected load from impedance and synchrotron radiation is indicated by the dashed line.

2. A dedicated feed-forward logic was integrated in the cryogenics control system. This applies regulations based on the measured properties of the circulating beam in order to minimize the temperature transients [15, 16].

The flexibility available in the design of the filling scheme was used to find the best compromise between the number of circulating bunches and the heat load in the arcs [17]. The characteristics of the different filling schemes used in Run 2 are illustrated in Fig. 5. The nominal filling scheme made of injections of 4×72 bunches was never accelerated to 6.5 TeV with the full number of bunches. In order to

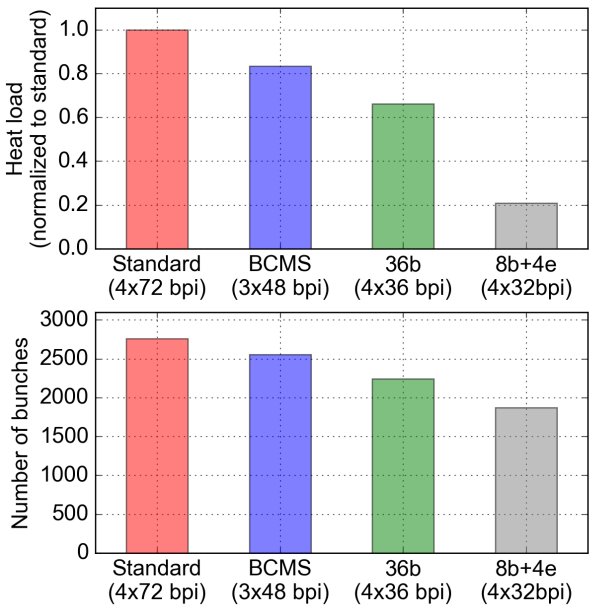

Figure 5: Heat load and number of bunches for different filling patterns used during Run 2.

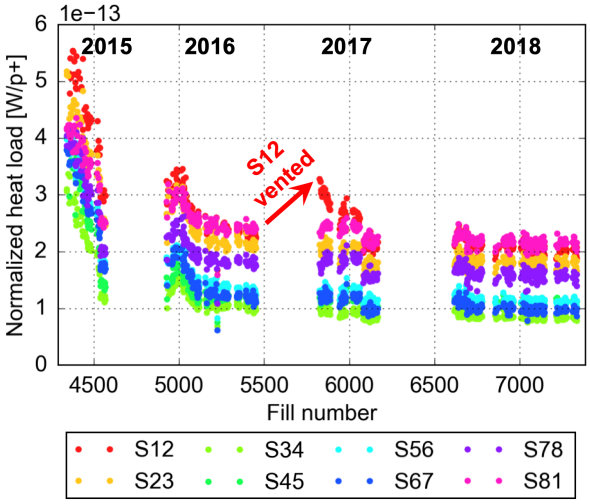

Figure 6: Evolution of the heat loads normalized to the bunch intensity in the eight LHC arcs during Run 2 (average over the arc half-cells). Data measured at 6.5 TeV for physics fills performed with the 25 ns bunch spacing and more than 600 bunches.

allow for the first physics fills with more than 2000 bunches in 2015, when the machine was not fully conditioned, a scheme made of injections of 4×36 bunches was used. In 2016, schemes made of trains of 48 bunches were adopted and were used for most of the luminosity production in the period 2016-18. This option is compatible with the high brightness production scheme in the injectors [11] and allows for significantly reduced heat loads compared to the standard scheme against a relatively small reduction of the number of bunches (-7 %). The "8b+4e" scheme, which strongly reduces the heat loads but allows only about 1900 bunches per beam, was used in the last part of the 2017 run in order to mitigate limitations arising from fast beam losses in the 16L2 arc-cell [18].

Surface conditioning also provided a significant mitigation of the heat loads. Figure 6 shows the heat loads measured in the eight sectors normalized to the circulating beam intensity, for all the physics fills of Run 2 that were performed with the 25 ns bunch spacing and with more than 600 bunches. A strong reduction of the heat loads, driven by surface conditioning, is observed in 2015 and in the first part of 2016. After that the heat loads remained practically constant, and the observed differences among sectors remained unaffected.

The arc heat loads directly affected LHC performance only in 2015. In the following years the LHC intensity reach was always limited by other factors, in particular by intensity limitations in the SPS in 2016, and by fast losses in the 16L2 arc cell in 2017-18 [18, 19].

Differences among the sectors

The heat loads are distributed very unevenly along the machine [20–22]. A dedicated inter-departmental Task Force has been formed to investigate this issue [23]. A detailed summary of the machine observations can be found in [22].

It is possible to identify two families within the eight arcs: a group of high-load sectors (including S12, S23, S78, S81) and a group of low-load sectors (including S34, S45, S56, S67). Interestingly, the high-load sectors are contiguous: in fact the machine is practically split in two parts.

Especially in the high-load sectors, large differences are observed also among half-cells, and between the two apertures of the same half-cell as shown in Fig. 7.

In most of the LHC arc half-cells temperature sensors are installed only at the entrance and at the exit of the cooling circuit, therefore only the total load deposited over the entire half-cell length is known. A small selection of arc half-cells have been equipped with additional thermometers to allow measuring the heat load on each magnet. In particular additional sensors have been installed in the cell 31L2, which happens to have a relatively high heat load. Figure. 8 illustrates the heat loads measured in this instrumented cell during a typical physics fill, showing that strong differences are present even between adjacent magnets.

A technique has been developed to further localize the heat source within the length of an individual magnet, based on the temperature transient observed after a beam dump [23]. Preliminary results show that the heat deposition is quite inhomogeneous also along the single beam screen. The accuracy and reliability of these measurements will improve after the Long Shutdown 2 (LS2), when direct measurements of the helium flow in the cooling circuit will become available [24].

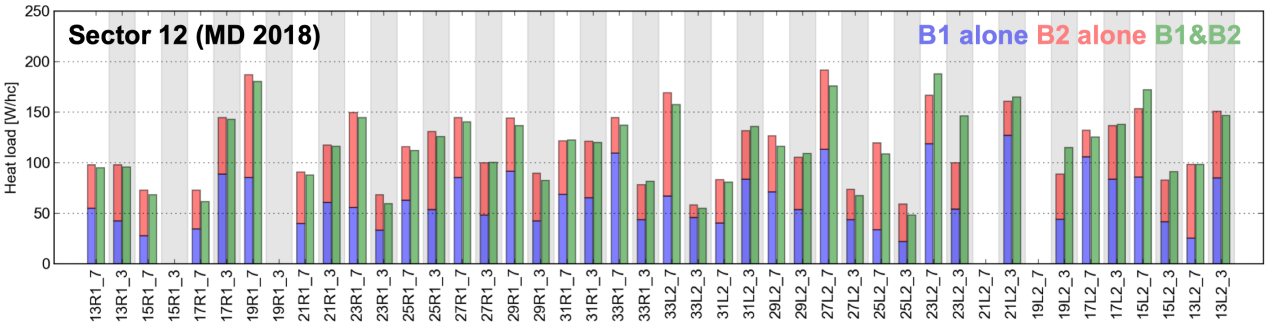

Figure 7: Heat loads measured in the half-cells of a high-load sector (S12) at 6.5 TeV, with beam 1 alone, beam 2 alone, and with the two beams circulating together.

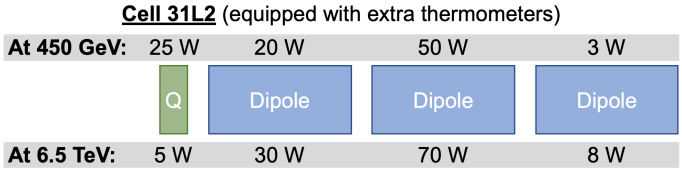

Figure 8: Heat loads measured on individual magnets in the instrumented half-cell 31L2 (corresponding to 31L2_3 in Fig. 7).

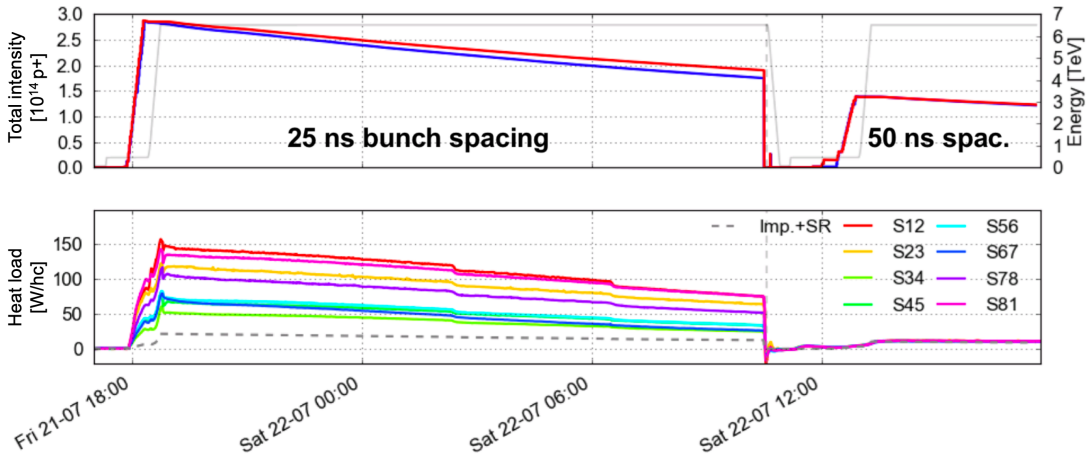

Figure 9: Intensities of the two LHC beams (top) and evolution of the heat load in the eight arcs (bottom) during two consecutive fills with different bunch spacing. Heat load values are in watts per half-cell. The expected load from impedance and synchrotron radiation is indicated by the dashed curve.

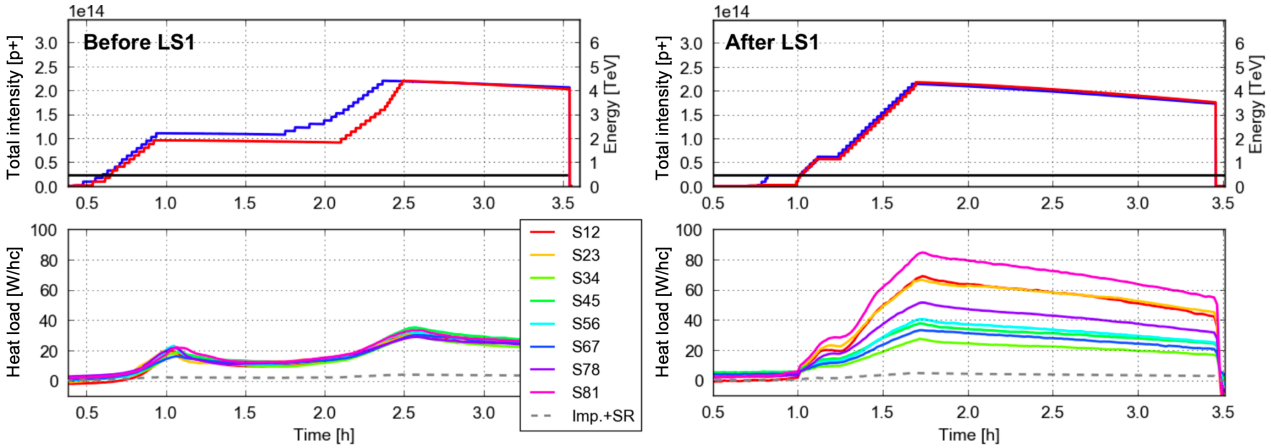

Figure 10: Beam intensities (top) and heat loads measured in the eight LHC arcs (bottom) during two fills conducted with the same filling pattern in 2012 (left) and in 2018 (right). Heat load values are in watts per half-cell.

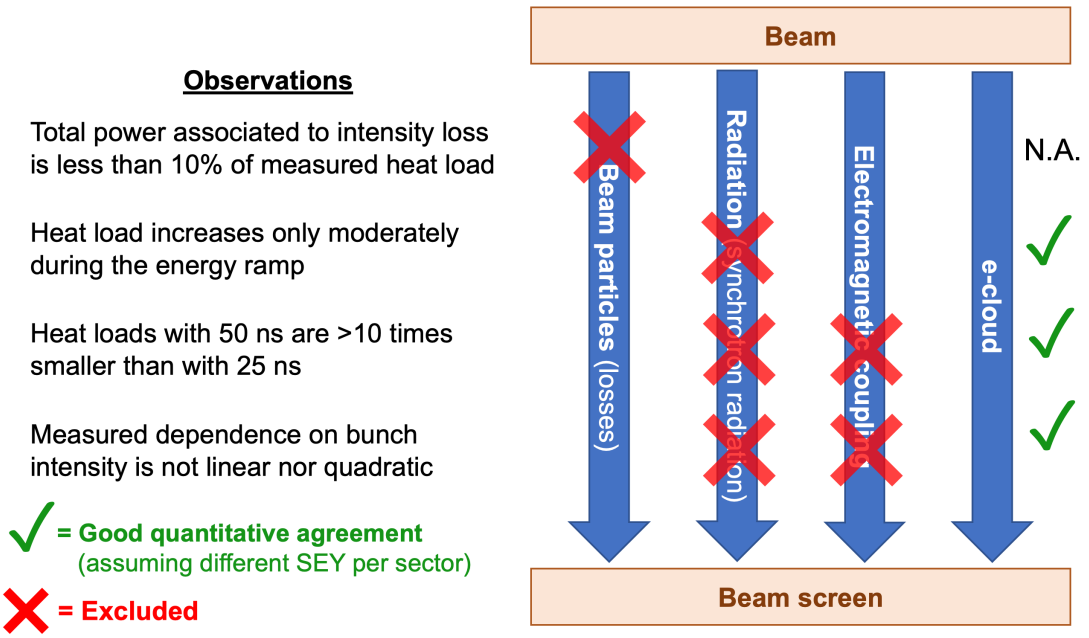

Figure 11: Compatibility of the available experimental observations with different mechanisms transferring power from the beam to the beam screen.

The most characteristic features of the observed heat loads are the following [20]:

- Heat loads significantly larger than impedance and synchrotron radiation estimate as well as differences among the eight sectors are very pronounced during operation with the 25 ns bunch spacing but disappear when the 50 ns bunch spacing is employed (as shown in Fig. 9).
- Heat load measurements taken with 25 ns beams at different bunch populations show a threshold around 0.4×10^{11} p/bunch.
- For a fixed bunch population the heat loads are proportional to the number of circulating bunch trains.
- Large heat loads and differences among sectors are already present at injection energy (450 GeV) and increase only moderately during the energy ramp.

Based on these features and on the analysis of the heat load measurement technique, it is possible to exclude that the observed differences result from measurement artifacts [20, 21].

Differences among sectors, half-cells and magnets are very reproducible and were observed in all 25 ns fills over the entire Run 2 (see for example Fig. 6 comparing the eight sectors). Nevertheless these differences were not always present. A test period with 25 ns beams took place at the end of Run 1, in 2012. The heat loads measured during this period can be directly compared against Run 2 data, as the measurement system was largely unchanged and the beam conditions were very similar [25]. A comparison between similar fills performed before and after LS1 is shown in Fig. 10. It is evident that the differences among sectors appeared only after the LS1, during which all arcs were warmed up to room temperature and exposed to air. It is possible to notice that still in 2018, after multiple years of conditioning of the beam chambers, the heat load in the worse sectors is four times larger than before LS1. So far, no difference in the activities conducted during LS1 in the eight sectors could be identified, which could explain this different behaviour in terms of heat load [23].

During Run 2, in particular during the 2016-17 winter shutdown, the sector 12 had to be warmed up to room temperature and exposed to air in order to replace a faulty main magnet. Interestingly this operation did not cause any permanent increase of the heat loads, contrary to what had been observed in LS1 [22].

Underlying mechanism

Experimental observations both from physics fills and from dedicated tests provide important information on the source of the heat loads and in particular of the observed differences among sectors.

It is possible to show that the power deposited in the form of the heat load ultimately comes from the beam. To do so, the power lost by the beam can be inferred from RF stable phase measurements and it is found to be consistent with heat load measurements from the cryogenics [20, 22].

Figure 11 illustrates different mechanisms that can transfer energy from the beam to the beam-screen and their compatiblity with the available experimental evidence [20, 21]:

- **Beam losses:** the hypothesis that the differences in heat loads are generated by protons lost on the beam screen,

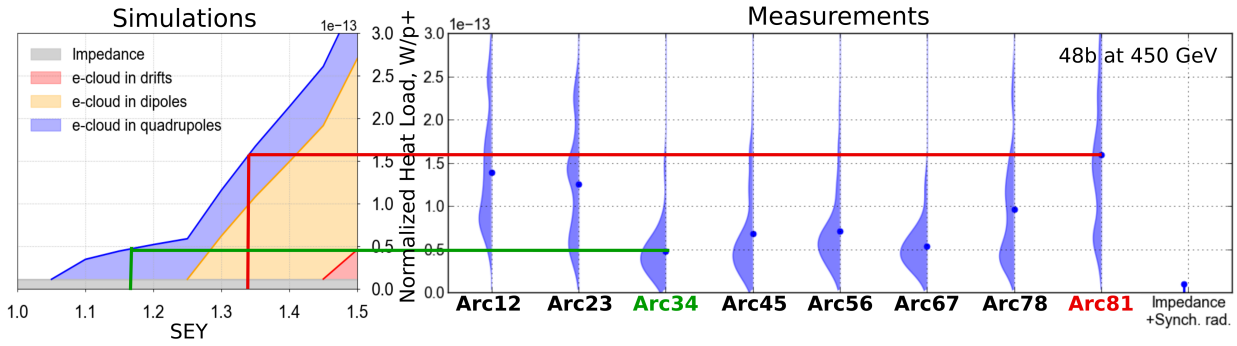

Figure 12: Left: simulated heat load per half-cell as a function of the SEY parameter for two circulating beams at 450 GeV (different contributions are shown in different colors). Right: corresponding measured heat loads. The curves represent the distribution among half-cells within each arc, the dots represent the average for each arc. The expected load from impedance and synchrotron radiation is shown on the right.

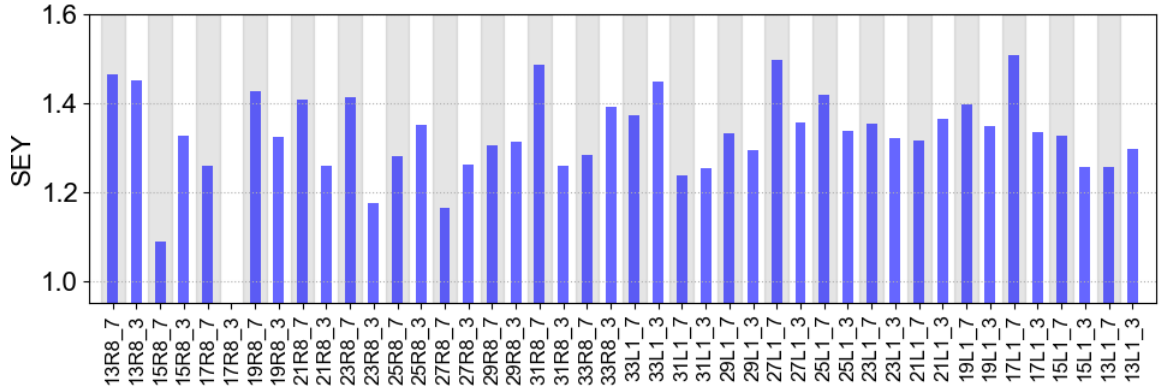

Figure 13: SEY parameter estimated for all cells in one of the sectors showing the highest heat load (S81).

can be easily discarded since the total power associated to beam losses (calculated from beam intensity measurements) only amounts to less than 10% of the measured heat loads.

- **Synchrotron radiation:** the possibility that the observed heat loads are deposited by photons radiated by the beam can also be excluded. In fact, the power from synchrotron radiation is proportional to the beam intensity and independent of the bunch spacing, which is inconsistent with the experimental observations (see for example Fig. 9). Finally a strong dependence on the beam energy would be expected, while only a small increase is observed during the energy ramp.

- **Beam coupling impedance:** the hypothesis that the energy is transferred through electromagnetic coupling between the beam and the surrounding structures is incompatible with the observations as well. The measured dependence of the heat load on the bunch intensity is not quadratic (see Fig. 18) and impedance heating cannot justify the large differences observed between 25 ns and 50 ns beams [26].

- **Electron cloud (e-cloud) effects**: the hypothesis that the energy deposition comes from e-cloud (electrons impacting on the beam pipe) is not in conflict with any of the mentioned observations. It can be further investigated by numerical simulations, as discussed in the following.

Comparison against e-cloud simulations

In order to compare the measured heat loads against e-cloud simulations, we assume that the differences observed among sectors and among half-cells are caused by non-identical surface properties resulting in a different Secondary Electron Yield (SEY) parameter (defined as $\delta_{\max}$ in [27]).

The e-cloud build-up process has been simulated using the PyECLOUD code [28] as a function of the SEY parameter for all the elements of the LHC arc half-cell. The simulation model is described in detail in [29]. The total simulated heat load as a function of the SEY is shown in Fig. 12 (left) for the two circulating 25 ns beams at 450 GeV, made of trains of 48 bunches. Figure 12 (right) shows the corresponding measured heat loads in the eight arcs. By comparing the two graphs, the SEY parameter corresponding to the average heat load in each arc can be determined, as illustrated in Fig. 12 for the sectors having the largest and the lowest heat loads. Likewise, based on the heat loads measured at each half-cell, the SEY distribution within the sectors can be found as shown in Fig. 13.

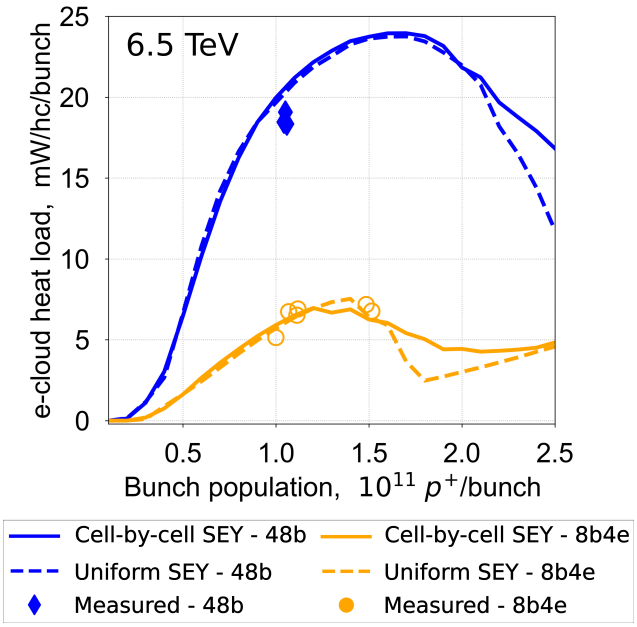

Figure 14: Heat loads per half-cell at 6.5 TeV as a function of the bunch intensity for one of the sectors showing the highest heat load (S81). Simulation results are represented by lines (continuous for the model assuming a different SEY in each half-cell, dashed for the simpler model assuming uniform SEY over the entire arc). Different filling patterns are shown in different colors.

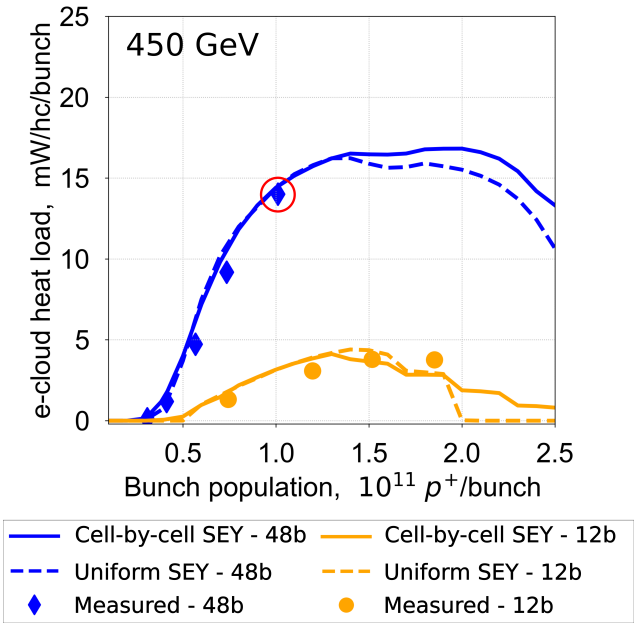

Figure 15: Heat loads at 450 GeV per half-cell as a function of the bunch intensity for one of the sectors showing the highest heat loads (S81). The data point used to infer the SEY is circled in red.

The SEY model defined in this way can be cross-checked against independent measurements. Using the obtained SEY parameters, we simulate the expected heat load as a function of the bunch population for different beam configurations (changing the bunch pattern and the beam energy). Figure 14 shows the expected dependence of the heat load on the bunch population at 6.5 TeV for one of the arcs with the largest heat load (S81). The results for the operational bunch pattern (trains of 48 bunches) and for the *8b+4e* scheme (trains of eight bunches separated by gaps of four empty slots) are shown in different colors. The dashed curves are calculated assuming uniform SEY along the arcs, estimated as described above using data collected at 450 GeV. The continuous curves, instead, are calculated assuming for each half-cell the SEY shown in Fig. 13. Measured data for both beam configurations are shown by the markers in Fig. 14. The agreement between measurements and simulations is found to be very good, especially for the sectors showing the highest heat load [30].

Systematic comparisons have been performed also at injection energy as shown in Fig. 15. The studies at 450 GeV focused in particular on the dependence of the heat loads on the bunch intensity, which will be discussed in more detail in the next section.

In general, it is possible to conclude that, not only is e-cloud heating the only identified mechanism that cannot be excluded based on the available observations, but it also allows achieving a good quantitative agreement between measurements and models, when assuming that the root cause of the differences in heat load is a difference in SEY.

Efforts are ongoing to identify possible causes that could alter the surface SEY. A laboratory measurement campaign has been launched by the TE-VSC team. In particular analyses and tests have been conducted on beam screens extracted from the LHC during the 2016-17 Extended Year-End Technical Stop and several alteration processes have been studied with laboratory experiments [31, 32]. An example is shown in Fig. 16, which illustrates the effect on the SEY conditioning of an improper rinsing of the products used for cleaning before their installation (which is nevertheless very unlikely to have happened). The history of the beam-screen manufacturing, preparation, installation and operation is also being analysed in detail, searching for possible causes of degradation, but no correlation has been found so far.

PLANS FOR LS2 AND OUTLOOK FOR RUN 3

Plans for LS2

Several actions are planned for the LS2 to improve the understanding on the observed limitations and prevent further increase of the heat loads:

- A different gas composition will be used for the venting of the arc beam vacuum system. This should allow a well controlled and reproducible exposure procedure [33];

- One magnet showing high heat load (namely the MB-B31L2, i.e. the dipole in the middle in Fig. 8) will be removed from the tunnel and will undergo extensive surface analysis. A direct comparison will be made

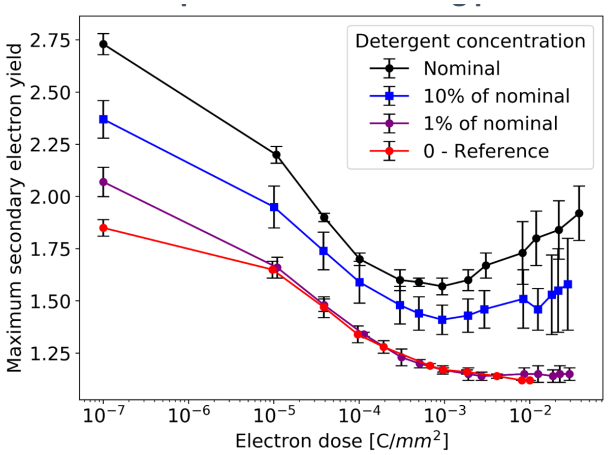

Figure 16: Results of laboratory conditioning experiments on beam screen surfaces exposed to different concentrations of detergent (courtesy V. Petit and M. Taborelli [32])

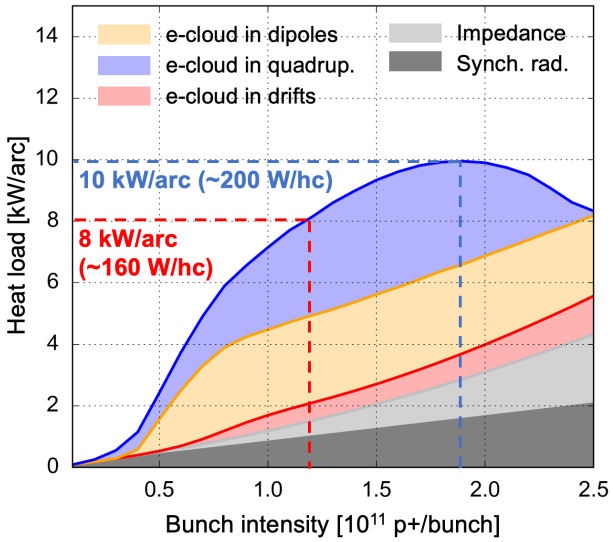

Figure 17: Heat load expected for the sector showing the highest load (S81) as a function of the bunch intensity, for a filling pattern with 2748 bunches in trains of 48 bunches.The different contributions are indicated in different colors. The nominal and measured capacity from the cryogenics are shown by the dashed lines.

against another magnet showing low heat load (namely the MB-C21R6) [34];

- New cryogenic instrumentation will be installed during LS2.
  In Run 3 a total of ten cells equipped with extra thermometers will be available (including the four presently available which will be upgraded). These cells will also be equipped with mass flow-meters to improve the precision of the measurement [24, 35].
  Additional instrumentation will be installed also to directly measure the global load on four arcs (S12, S23, S56, S67) [24].

- BE-BI will continue the development of a microwave-based technique for direct measurement of the e-cloud density in selected half-cells [36].

Heat load dependence on bunch intensity and expected intensity reach

During Run 3, with the commissioning of the LHC Injectors Upgrade, it will become possible to gradually increase the bunch intensity [37]. A realistic target could be to establish operation with 2748 bunches per beam with 1.8×10^{11} p/bunch by the end of Run 3 [38].

Figure 17 shows the expected dependence of the heat load on the arc beam screens on the circulating bunch intensity, for the sectors having highest heat loads, assuming 2748 bunches per beam in trains of 48 bunches. The contributions from impedance and synchrotron radiation are estimated using analytical formulas [39], while the contributions from the e-cloud in the dipole, quadrupole and drift regions are estimated by macroparticle simulations, using the model defined in the previous section (SEY_{max}=1.35). The models predict a relatively mild increase of the heat loads for bunch intensities above 1.2×10^{11} p/bunch, due to the fact that the contributions from e-cloud are not expected to increase significantly above such value.

Direct experimental checks above 1.2×10^{11} p/bunch were not possible in Run 2 using long bunch trains, due to intensity limitations in the injectors (mainly from RF power limitations in the SPS) [11, 37]. Towards the end of 2018, trains of 12 bunches with high bunch intensity (up to 1.9×10^{11} p/bunch) became available from the SPS and could be used for tests in the LHC during the last proton Machine Development block before LS2. The results of those experiments are shown in Fig. 18. Measurements were taken in four different fills at injection energy, each performed with a different bunch intensity in the range $0.4 - 1.9 \times 10^{11}$ p/bunch. The data clearly shows that the heat loads from e-cloud tend to saturate above 1.5×10^{11} p/bunch. When comparing the measurement results against simulations, very good agreement is found especially for the high-load sectors as shown in Fig. 15 [30].

Beam induced heat loads in the arc beam screens can pose limitations on the LHC intensity reach in Run 3. Assuming that a filling scheme made of trains of 48 bunches will be employed to fill the machine with 2748b, and assuming the design cooling capacity from cryogenics of 8 kW/arc (corresponding to 160 W/half-cell) [1], we observe that the bunch intensity would be limited to about 1.3×10^{11} p/bunch (see Fig. 17).

During Run 2, the LHC cryogenics has been operated in an optimized configuration (using one cold-compressor unit to serve two consecutive sectors) profiting from the lower-than-expected heat loads at 1.9 K. The cryoplants feeding the high-load sectors have been recently characterized by the cryogenics team, and they were found to have a better than expected performance, being able to deliver 10 kW/arc [40]. Comparing this value with the simulated heat loads in Fig. 17,

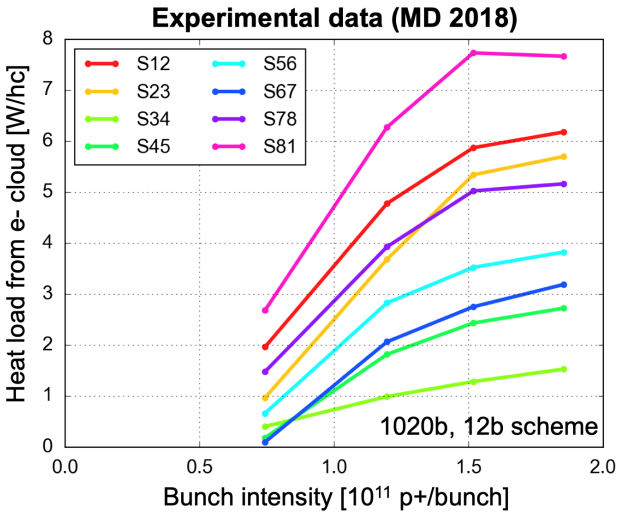

Figure 18: Heat loads measured for different bunch intensities at 450 GeV in the eight LHC arcs using trains of 12 bunches. The load expected from impedance and synchtrotron radiation is subtracted.

we observe that a bunch intensity of 1.8×10^{11} p/bunch could be within reach, assuming that no further degradation takes place in LS2 and that the cryoplants can deliver reliably 10 kW/arc.

In case of issues, like further degradation in LS2, power limitations from the cryoplants, or worse than expected dependence of the heat loads on bunch intensity, the heat loads will need to be mitigated using the 8b+4e filling pattern. "Mixed filling schemes" featuring 8b+4e trains and 25 ns trains within the same scheme can also be used to maximize the number of bunches without exceeding the heat load limit defined by the cryoplant performance [41].

First thoughts on scrubbing after LS2

During LS2 most of the beam chambers will be exposed to air, including the arc beam screens, therefore the conditioning accumulated during Run 2 will be lost and the situation at the beginning of the 2021 run will be similar to the one observed at the beginning of 2015.

A period dedicated to scrubbing at 450 GeV will have to be allocated at the beginning of the 2021 run with the main objective of mitigating the e-cloud formation to an extent sufficient to control transverse instabilities and allow physics operation with 25 ns beams.

In 2015, about 16 days of beam time dedicated to scrubbing were needed (long faults as well as other tests and activities are subtracted from this day count). During that period several issues were encountered, which were limiting the conditioning pace. All of them have been mitigated during Run 2 and LS2, in particular:

- The TDI injection absorbers, which were limiting the intensity due to vacuum issues, will be replaced with redesigned devices (TDIS) during LS2 [42];
- The pressure rise in the injection kicker (MKI) region has been mitigated by upgrading the pumping system during Run 2. Alumina tubes with a special coating to reduce the electron multipacting will be tested in some of the MKI modules [42];
- The sensitivity to heat load transients leading to loss of cryogenics conditions has been mitigated by redefining the "CryoMaintain" rules and by developing a dedicated feed-forward control (as discussed before);
- The optimized tune settings identified in Run 2, allow a more effective use of octupoles and chromaticity to control transverse instabilities [9].

Thanks to these measures the scrubbing process is expected to be more efficient in 2021 compared to 2015 and therefore less time will be required.

As in Run 2, after the scrubbing run further conditioning will need to be accumulated with physics operation with 25 ns, in order to further mitigate the arc heat loads and allow gradually increasing the circulating beam intensity.

SUMMARY

During Run 2 beam-induced scrubbing allowed mitigating to a large extent the detrimental effects of e-cloud, enabling the exploitation of 25 ns beams for luminosity production. Nevertheless e-cloud effects could not be fully suppressed and continued affecting beam stability and beam parameters evolution during the entire Run 2.

Electrons impacting on the beam screens caused large heat loads, which constituted a significant challenge for the cryogenic system. This was partially mitigated by optimizing the filling scheme and by the parasitic conditioning accumulated during physics fills. Moreover a cooling capacity larger than foreseen by design became available for the beam screens thanks to an optimized configuration of the cryogenic system (profiting from the lower than expected loads at 1.9 K).

Large differences in heat load were observed among the eight LHC sectors. These differences were not present during Run 1 (also during tests done with 25 ns beams). The only identified heating effect that is compatible with observations is the e-cloud. It is possible to reproduce the observed heat load with numerical simulations by assuming that some surface modification leading to high SEY took place in LS1. This hypothesis is being followed up by laboratory studies. During LS2 beam-screens will be extracted and analyzed, new instrumentation will be installed and precautions will be taken to avoid further degradation.

In 2018 the dependence of e-cloud on the bunch intensity was probed experimentally with short trains up to 1.9e11 p/b. The observed trend was found to be consistent with models. Based on these results, assuming no further degradation in LS2 and counting on cryo-plants performing better than designed (as measured), physics operation with 1.8×10^{11} p/bunch could be within reach for Run 3.

ACKNOWLEDGMENTS

The authors would like to thank all members of the CERN Beam-Induced Heat Loads Task Force, G. Arduini, F. Gior-

dano, E. Métral, V. Petit, B. Salvant, and M. Taborelli for their important input to the present contribution.

REFERENCES

[1] O. Bruning, P. Collier, P. Lebrun, S. Myers, R. Ostojic, J. Poole, and P. Proudlock (editors), "LHC Design Report, Volume 1." CERN-2004-003-V-1, 2004.

[2] G. Rumolo, "Electron cloud effects in the LHC in 2011." in *Proceedings of the 3rd Evian Workshop, Evian 12 - 14 Dec 2011*, CERN-ATS-2012-083.

[3] G. Iadarola, "Electron cloud and scrubbing in 2012 in the LHC." in *Proceedings of the 4th Evian Workshop, Evian 17-20 Dec 2012*, CERN-ATS-2013-045.

[4] G. Iadarola, " Electron cloud and scrubbing: perspective and requirements for 25 ns operation in 2015." in *Proceedings of the 5th Evian Workshop, Evian 2-4 June 2014*, CERN-ACC-2014-0319.

[5] O. Domínguez, K. Li, G. Arduini, E. Métral, G. Rumolo, F. Zimmermann, and H. M. Cuna, "First electron-cloud studies at the large hadron collider," *Phys. Rev. ST Accel. Beams*, vol. 16, p. 011003, Jan 2013.

[6] G. Iadarola, "Performance limitations from electron cloud in 2015." in *Proceedings of the 6th Evian Workshop, Evian 15-17 Dec 2015*, CERN-ACC-2015-376.

[7] L. Mether, "Electron cloud in 2016: cloudy or clear?." in *Proceedings of the 7th Evian Workshop, Evian 13-15 Dec 2016*, CERN-ACC-2017-094.

[8] X. Buffat *et al.*, "Transverse instabilities." These proceedings.

[9] A. Romano, G. Iadarola, K. Li, and G. Rumolo, "Macroparticle Simulation Studies of the LHC Beam Dynamics in the Presence of Electron Cloud," in *Proceedings, 8th International Conference, IPAC 2017, Copenhagen, Denmark, May 14-19, 2017*, p. TUPVA018, 2017.

[10] S. Kostoglou *et al.*, "Luminosity, lifetime and modelling." These proceedings.

[11] H. Bartosik *et al.*, "Injectors beam performance evolution during run 2." These proceedings.

[12] A. Romano, O. Boine-Frankenheim, X. Buffat, G. Iadarola, and G. Rumolo, "Electron cloud buildup driving spontaneous vertical instabilities of stored beams in the large hadron collider," *Phys. Rev. Accel. Beams*, vol. 21, p. 061002, Jun 2018.

[13] G. Ferlin, "Analysis of the beam screen temperature transients and related operational issues." Presentation at the LHC Machine Committee, CERN, 23 Sep 2015, available at https://indico.cern.ch/event/447445/.

[14] P. Chiggiato, "Can we increase the temperature of the bs cooling?." Presentation at the LHC Machine Committee, CERN, 23 Sep 2015, available at https://indico.cern.ch/event/447445/.

[15] B. Bradu, A. Tovar González, E. Blanco Viñuela, P. Plutecki, E. Rogez, G. Iadarola, G. Ferlin, and B. Fernández Adiego, "Compensation of beam induced effects in LHC cryogenic systems," in *Proceedings of International Particle Accelerator Conference (IPAC'16), Busan, Korea, May 8-13, 2016*, 2016.

[16] G. Iadarola, B. Bradu, P. Dijkstal, L. Mether, and G. Rumolo, "Impact and Mitigation of Electron Cloud Effects in the Operation of the Large Hadron Collider," in *Proceedings, 8th International Particle Accelerator Conference (IPAC 2017): Copenhagen, Denmark, May 14-19, 2017*, p. TUPVA019, 2017.

[17] G. Iadarola, "Filling schemes and e-cloud constraints." in *Proceedings of the 7th Evian Workshop, Evian 13-15 Dec 2016*, CERN-ACC-2017-094.

[18] L. Mether, "16l2: operation, observations and physics aspects." in *Proceedings of the 8th Evian Workshop, Evian 12 - 14 Dec 2017*, CERN-ACC-2019-012.

[19] D. Mirarchi *et al.*, "Special losses." These proceedings.

[20] G. Iadarola, "Electron cloud and heat loads in the LHC arcs." Accelerator and beam physics forum, CERN, 12 Jul 2018 https://indico.cern.ch/event/740046.

[21] G. Iadarola, "Heat loads in the lhc arcs: observations and comparison against models." Presentation at the LHC Machine Committee, CERN, 29 Aug 2018 , available at https://indico.cern.ch/event/754131/.

[22] G. Iadarola, G. Rumolo, P. Dijkstal, and L. Mether, "Analysis of the beam induced heat loads on the LHC arc beam screens during Run 2," *CERN-ACC-NOTE-2017-0066*, Dec 2017.

[23] L. Tavian, "Report from the task force on beam induced heat load." Presentation at the LHC Performance Workshop 2018, Chamonix, Jan 2018.

[24] L. Tavian, "Heat load task force: Additional instrumentation." Presentation at the LMC Machine Committee, CERN, 12 Sep 2018, available at https://indico.cern.ch/event/756727.

[25] G. Iadarola, "Head loads in run 1 and run 2." Presentation at the LHC Machine Committee, CERN, 12 Sep 2018 , available at https://indico.cern.ch/event/756722/.

[26] F. Giordano and B. Salvant, "Impedance considerations on the measured heat loads." Presentation at the Electron Cloud Meeting, CERN, 25 Aug 2017. https://indico.cern.ch/event/660465/.

[27] R. Cimino, I. R. Collins, M. A. Furman, M. Pivi, F. Ruggiero, G. Rumolo, and F. Zimmermann, "Can low-energy electrons affect high-energy physics accelerators?," *Phys. Rev. Lett.*, vol. 93, p. 014801, Jun 2004.

[28] G. Iadarola, E. Belli, K. Li, L. Mether, A. Romano, and G. Rumolo, "Evolution of Python Tools for the Simulation of Electron Cloud Effects," in *Proceedings, 8th International Particle Accelerator Conference (IPAC 2017): Copenhagen, Denmark, May 14-19, 2017*, p. THPAB043, 2017.

[29] P. Dijkstal, G. Iadarola, L. Mether, and G. Rumolo, "Simulation studies on the electron cloud build-up in the elements of the LHC Arcs at 6.5 TeV," *CERN-ACC-NOTE-2017-0057*, Oct 2017.

[30] G. Skripka, "Scaling of ecloud effects with bunch population." Presentation at the HiLumi WP2 Meeting, CERN, 5 Mar 2019, available at https://indico.cern.ch/event/800616/.

[31] V. Petit, "Sey measurements of the arc 1-2 removed-magnet beam screen." Presentation at the LMC Machine Committee, CERN, 5 Apr 2018, available at https://indico.cern.ch/event/629710/.

[32] V. Petit, "Status of understanding of mechanisms of conditioning/deconditioning of beam screens." Presentation at the LMC Machine Committee, CERN, 7 Nov 2018, available at https://indico.cern.ch/event/771601/.

[33] G. Bregliozzi, "Beam screen venting procedure for ls2." Presentation at the LMC Machine Committee, CERN, 12 Dec 2018, available at https://indico.cern.ch/event/780656.

[34] M. Taborelli, "Status of understanding of mechanisms of conditioning/deconditioning of beam screens." Presentation at the LMC Machine Committee, CERN, 6 Mar 2019, available at https://indico.cern.ch/event/803742.

[35] B. Bradu *et al.*, "Additional cryogenic instrumentation for local diagnostics of beam-induced heat loads." Engineering Change Request, 2019. https://edms.cern.ch/document/2045687/1.0.

[36] M. Wendt, "Results on e-cloud density measurement." Presentation at the Task Force on beam-induced heat loads meeting, CERN, 28 Nov 2018, available at https://indico.cern.ch/event/776322/.

[37] G. Rumolo *et al.*, "What to expect from the injectors during run 3." These proceedings.

[38] N. Karastathis *et al.*, "Report from the run 3 configuration working group." These proceedings.

[39] G. Iadarola, E. Metral, and G. Rumolo, "Beam induced heat loads on the beam-screens of the twin-bore magnets in the IRs of the HL-LHC." CERN-ACC-2016-0112, 2016.

[40] G. Ferlin *et al.*, "Cryogenics." These proceedings.

[41] G. Iadarola, "Digesting the LIU high brightness beam: is this an issue for HL-LHC?." Presentation at the LHC Performance Workshop 2018, Chamonix, Jan 2018.

[42] F. Velotti *et al.*, "Injection systems." These proceedings.